

Phonon Instabilities in fcc and bcc Tungsten

K. Einarsdotter, B. Sadigh, G. Grimvall, and V. Ozoliņš*

Department of Theoretical Physics, Royal Institute of Technology, SE-100 44 Stockholm, Sweden
(Received 11 June 1997)

The lattice dynamics of bcc and fcc W is studied as a function of pressure using the density-functional linear-response theory. At high pressures and $T = 0$ K, bcc W has a higher enthalpy than the fcc and hcp phases and it develops phonon softening anomalies related to this thermodynamic instability; however, it remains dynamically stable. In contrast, the widely unstable shear modes of fcc W at zero pressure (when $H_W^{\text{fcc}} > H_W^{\text{bcc}}$) stabilize with increasing pressure before $H_W^{\text{fcc}} < H_W^{\text{bcc}}$. Hence the thermodynamic and dynamic instabilities are uncorrelated. [S0031-9007(97)04061-1]

PACS numbers: 63.20.Dj, 62.20.Dc, 71.15.Mb, 71.20.Be

Dynamical instabilities or anomalous softening in the lattice vibrations of metals in the bcc and fcc structures are of considerable current interest [1–8]. They may occur for wavevectors well into the first Brillouin zone (BZ), as is exemplified for many metals in the bcc structure by the longitudinal phonon mode at $\mathbf{q} = [\frac{2}{3}\frac{2}{3}\frac{2}{3}]$ [1,2], transforming bcc into the ω phase for sufficiently large amplitude. In other cases the instability is due to a negative elastic constant for shear modes, often related to the martensitic transformation between fcc and bcc structures via the tetragonal Bain's path [3–6]. Reference to dynamical instabilities recently clarified a long-standing discrepancy between the structural energy differences obtained from *ab initio* electron structure calculations and those derived through a Calphad analysis of binary phase diagrams [3,4,7]. Tungsten is then a typical example. The stable phase has the bcc lattice structure while fcc W is dynamically unstable. *Ab initio* calculations [7] showed that the elastic constants C_{44} and $C' = (C_{11} - C_{12})/2$ are both negative, implying that fcc W is dynamically unstable under *all* elastic shear, while some BZ boundary phonons were found to be stable.

The importance of lattice instabilities in materials science, and the unusual features occurring in W, motivates a detailed *ab initio* calculation of the lattice dynamics for this metal, both in the unstable fcc phase and in the stable bcc phase. It has been speculated that the dynamical instability of W at $T = 0$ may be stabilized at high T , a possibility which would have profound implications for the thermodynamic Calphad-type analysis of fcc-based W alloys. One then refers to, e.g., the $L[\frac{2}{3}\frac{2}{3}\frac{2}{3}]$ mode in bcc Ti and Zr [1,2,9], which is unstable at low T but is stabilized at high T . However, such a behavior is unlikely if the unstable phonon modes occur in a large part of the BZ. Therefore we will map out that region in the BZ where the fcc-W phonons are dynamically unstable and study how it changes with pressure. We also perform calculations for the stable W bcc phase, compare with experiments, and pay particular attention to incipient instabilities under an applied pressure when bcc W becomes *thermodynamically* unstable (i.e., has a higher

Gibbs energy) with respect to more close-packed phases (e.g., fcc and hcp).

We use density-functional theory [10] in the local density approximation [11]. The calculations are performed using a plane-wave basis set and norm-conserving pseudopotentials for W $5s, 5p, 6s, 6p$ and $5d$ states as valence states. The core radii are chosen to be 2.0 a.u. We use two nonlocal separable projectors for s and p channels, and apply the optimization technique of Ref. [12] to deal with the localized $5s, 5p$ and $5d$ states. It allows a cutoff energy $E_{\text{cut}} = 22.5$ Ry, and a total energy convergence with respect to the basis, better than 0.1 mRy/atom. The BZ summations are carried out on a $16 \times 16 \times 16$ Monkhorst-Pack [13] grid using the first-order Methfessel-Paxton broadening scheme [14] with $W = 20$ mRy. The phonon frequencies are calculated using the density functional linear response method [15] for metallic systems [16,17]. These calculations are performed for phonon wave vectors on the same reciprocal space mesh as used in the BZ summations.

Using the parameters above we obtain equilibrium volumes $V_0 \equiv V_{\text{fcc}}^{\text{calc}} = 15.52 \text{ \AA}^3/\text{atom}$ and $V_{\text{bcc}}^{\text{calc}} = 15.19 \text{ \AA}^3/\text{atom}$ for fcc and bcc W, respectively (experiments [9] give $V_{\text{bcc}}^{\text{exp}} = 15.78 \text{ \AA}^3/\text{atom}$). From the calculated binding energy curves for bcc, fcc, and hcp W, we find that the fcc phase becomes more stable than bcc at 11 Mbar. The enthalpy of hcp W becomes lower than the enthalpy of bcc W at 12 Mbar, but the former is higher than the enthalpy of fcc W at all pressures considered. Volume differences between these phases at constant pressure are smaller than 1.5%.

Figure 1 shows calculated phonon dispersion curves $\nu(\mathbf{q})$ at the volume V_0 , and experimental results [18]. The agreement with experiment is very good (deviations $\leq 6\%$), characteristic of first-principles LDA calculations of this kind. (Interestingly, the deviation is largest along the HP direction in Fig. 1, where we also note a significant volume dependence even near $V = V_0$, see Figs. 2 and 3.) Our calculations reproduce an interesting feature of the experimental phonon dispersion—the near degeneracy and crossing of the transversal modes along

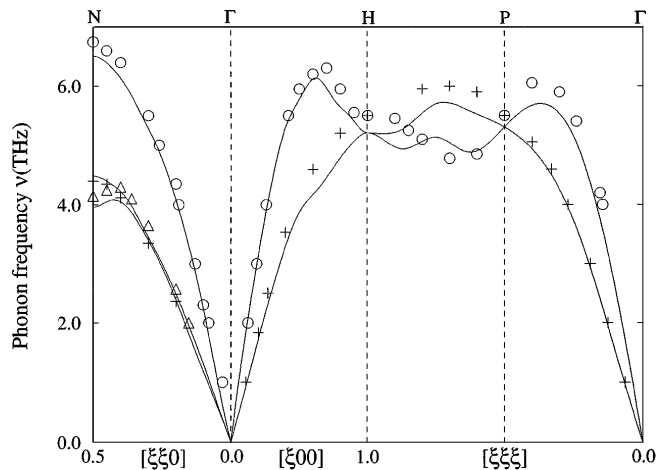


FIG. 1. Experimental [18] (symbols) and calculated (solid lines) phonon frequencies of bcc W at the volume V_0 .

$[\xi\xi0]$. From a smooth polynomial fit to $\nu(\mathbf{q})$ at different volumes, we calculate the Grüneisen parameters $\gamma_G(\mathbf{q}) = -(\partial \ln \nu(\mathbf{q}) / \partial \ln V)$ for bcc W when $V = V_0$, and average it over the BZ using the method of Mauri *et al.* [8] to get $\gamma_G = 1.5$. The electronic contribution to γ_G , obtained through the calculated $\partial \ln N(E_F) / \partial \ln V$ [$N(E_F)$ is the density of states at the Fermi level], was found to be slightly less than 0.1. The experimental thermodynamic Grüneisen parameter is $\gamma_G = 1.6$ for bcc W at 300 K [19], in excellent agreement with our calculated average phonon part. We conclude that our pseudopotential method accurately predicts the phonon frequencies and their volume dependence for bcc W.

We next study fcc and bcc W at high pressures, when bcc W has a higher Gibbs energy than the close-packed

fcc and hcp phases. It is interesting to see if the phonons and elastic constants of bcc W exhibit anomalies indicative of its thermodynamic instability at high pressures (recall that fcc W at zero pressure is both *thermodynamically* and *dynamically* unstable). We also investigate the gradual dynamic stabilization of fcc W with pressure.

The calculated phonon dispersion curves of bcc W at several pressures are shown in Fig. 2, and Table I gives the elastic constants of fcc and bcc W. We see that bcc W is dynamically stable [$\nu(\mathbf{q})^2 > 0$ and $C_{ij} > 0$] at all the volumes considered, even though it is thermodynamically unstable at $V = 0.442V_0$ (at $P = 12$ Mbar and $T = 0$ K, corresponding to bcc volume $0.438V_0$, both fcc and hcp W are predicted to have a lower enthalpy than bcc W). In order to see incipient instabilities more clearly, we rescale the dispersion curves at different atomic volumes so that the maximum frequency of each branch (longitudinal or transversal) becomes volume independent. Figure 3 shows the result for branches and directions where anomalies are observed. Strong softening with decreasing volume occurs around the $L[\frac{2}{3}\frac{2}{3}\frac{2}{3}]$ mode. We interpret this as a manifestation of the inherent softness of that mode which follows from geometrical arguments [20] (connection between the bcc and ω structures for sufficiently large displacements), and is observed, e.g., in the bcc structures β -Sc, β -Ti, and V [1,2,9]. We also note a smaller but significant softening in the entire transverse branch along $[\xi\xi0]$ with the polarization vector along $[1\bar{1}0]$. The long wavelength modes of this branch correspond to the C' elastic constant, responsible for transition to the fcc structure through Bain's path. The $T_{[1\bar{1}0][\frac{1}{2}\frac{1}{2}0]}$ mode has previously been studied in several systems [1,21,22], since it was conjectured that it gives a possible path for martensitic bcc \rightarrow hcp transformations. An interesting feature is the relative softening of the $T_{[1\bar{1}0][\frac{1}{4}\frac{1}{4}0]}$ phonon frequency compared to the $T_{[1\bar{1}0][\frac{1}{2}\frac{1}{2}0]}$ mode. From a geometrical consideration we find that the former, if unstable, provides

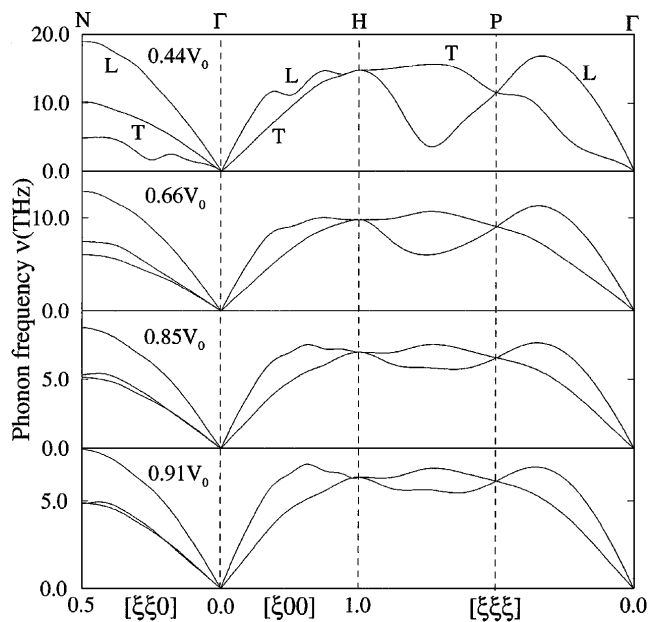


FIG. 2. Calculated phonon frequencies of bcc W at different volumes, corresponding to the pressures 12 Mbar, 3 Mbar, 0.6 Mbar, and 0.3 Mbar, respectively.

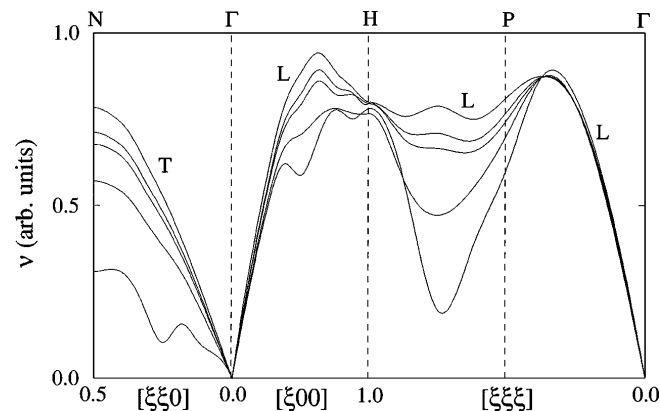


FIG. 3. Calculated phonon dispersion curves for selected branches of bcc W at several volumes, scaled to a common maximum frequency ($\nu_L^{\max} = 18.9$ THz for longitudinal and $\nu_T^{\max} = 15.7$ THz for transversal modes).

TABLE I. Calculated elastic constants for fcc and bcc W.

		V_0	$0.854V_0$	$0.656V_0$	$0.442V_0$
bcc	C' (Mbar)	1.74	2.45	2.67	3.61
	C_{44} (Mbar)	1.49	2.28	4.92	11.24
	B (Mbar)	0.32	0.57	13	37
fcc	C' (Mbar)	-1.59	-1.34	-0.81	5.52
	C_{44} (Mbar)	-1.28	0.76	3.15	14.41
	B (Mbar)	0.30	0.57	12	36
	$\Delta E^{\text{fcc/bcc}}$ (mRy/atom)	37.1	42.0	40.1	-4.21

a transition path from the bcc to the hcp structure, similar to that involving the $T_{[1\bar{1}0]}[\frac{1}{2}\frac{1}{2}0]$ mode. Hence, the softening of $T_{[1\bar{1}0]}[\frac{1}{2}\frac{1}{2}0]$ and $T_{[1\bar{1}0]}[\frac{1}{4}\frac{1}{4}0]$ is related.

We now turn to instabilities in the fcc W; see Table I and Fig. 4 where $-\nu$ is plotted when $\nu^2(\mathbf{q}) < 0$. At normal pressure all long wavelength transverse modes are unstable and the dynamical instability extends far into the BZ. A strong softening anomaly occurs in the lower transverse $[\xi\xi 0]$ branch with polarization along $[1\bar{1}0]$. We note that the long wavelength $T_{[001]}[\xi\xi 0]$ modes, corresponding to C_{44} , are stabilized at the volume $0.854V_0$, while C' is still unstable at $0.656V_0$. Another important feature is seen in the transverse $[\xi\xi 0]$ branches. The $T_{[1\bar{1}0]}[\xi\xi 0]$ mode has an instability at finite wavelengths, although the long wavelength part, corresponding to the elastic constant C' , is stable (see the panel for $V = 0.656V_0$). This means that a C' -related Bain's path is not necessarily responsible for a dynamical instability of the fcc phase. A different behavior is observed in the $T_{[001]}[\xi\xi 0]$, $T[\xi\xi\xi]$ and $L[\xi 00]$ modes where the instabilities are first developed in the long wavelength limit, being caused by negative elastic constants.

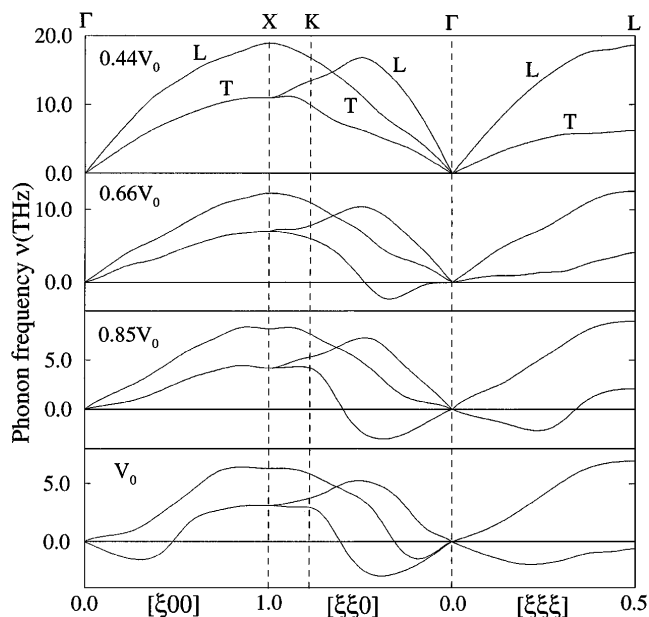


FIG. 4. Calculated phonon frequencies for fcc W at pressures 12 Mbar, 3 Mbar, 0.6 Mbar, and 0 Mbar, respectively.

A remarkable feature in fcc W is demonstrated by the $T[\xi\xi\xi]$ branch which is weakly unstable at V_0 for all wave vectors \mathbf{q} out to the BZ boundary. This branch remains soft over a large variation in volume, and its maximum frequency is always smaller by at least a factor of two, compared with all other branches. In analogy to a qualitative reasoning of Mauri *et al.* [8] for a pressure-induced softening in tellurium, we write the frequencies of this branch as a “normal” (n) and an “anomalous” (a) part; $\nu^2(\mathbf{q}) = \nu_n^2(\mathbf{q}) + \nu_a^2(\mathbf{q})$. We expect ν_n (due to short-range force constants) to be similar in shape to the corresponding branch in fcc copper [9], which is free of softening anomalies. If we now normalize $\nu^2(\mathbf{q})$ to take the value 1 at the X point in the BZ and scale it accordingly for shorter \mathbf{q} , we get the result in Fig. 5. We see how the large dip caused by the “anomalous” contribution $\nu_a^2(\mathbf{q})$ gradually decreases with decreasing atomic volume. This indicates that the dynamical instability of this branch is caused by a long-range contribution to $\nu^2(\mathbf{q})$, possibly from anomalous electronic screening effects.

Finally, we analyze the connection (if any) between the thermodynamic and dynamic instabilities in fcc and bcc W. Figure 6 gives the total energy $E(c/a)$ along the (a) tetragonal and (b) trigonal Bain's paths at several volumes. As explained in Ref. [4], $E(c/a)$ as a function of c/a has at least three extrema. Two of them occur at the points of cubic symmetry. For the tetragonal Bain's path, the third extremum is a minimum and is located

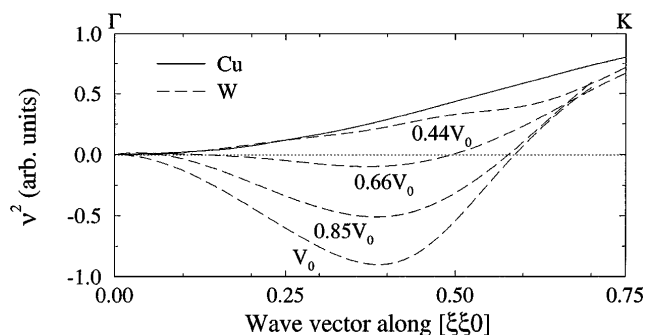


FIG. 5. Square of the phonon frequencies $\nu^2(\mathbf{q})$ for the transversal $T_{[1\bar{1}0]}[\xi\xi 0]$ branch of Cu [9] and our calculated results for fcc W. All curves are normalized to 1 at the X point.

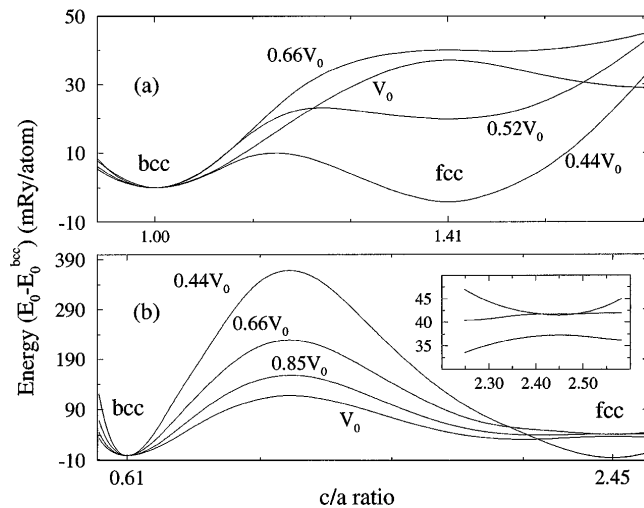


FIG. 6. (a) Tetragonal and (b) trigonal Bain's paths between fcc and bcc W. The inset in (b) shows the region around fcc W.

at $c/a > 1$. As the volume decreases, the position of this minimum moves toward smaller c/a (higher close-packing), eventually merging with the fcc maximum into an inflection point [Fig. 6(a)]. At further volume decrease the fcc structure represents a locally stable minimum, and the third extremum is a maximum located between the bcc and fcc c/a values. We note that C' [given by the curvature of $E(c/a)$ in Fig. 6(a)] is stabilized *before* the fcc phase becomes thermodynamically stable. The trigonal Bain's path [Fig. 6(b)] at zero pressure ($V = V_0$) has *five* extrema (i.e., two more than required), and fcc W is a locally unstable phase. Already at $V = 0.854V_0$ both extra minima have merged with the fcc maximum, stabilizing C_{44} for fcc W. Due to the high energy barrier separating bcc and fcc W along the trigonal path, C_{44} is rapidly increasing with pressure in both structures. Furthermore, the bcc phase is dynamically stable ($C' > 0$ and $C_{44} > 0$) even when fcc W has a lower energy at $V = 0.442V_0$. From Fig. 6 it appears that there is no direct connection between the thermodynamic and long-wavelength dynamic instabilities in the case of W under pressure.

In conclusion, the present *ab initio* calculation of phonon frequencies is the most detailed that has been performed for a transition metal. We obtained an excellent agreement with the experimental phonon frequencies and the Grüneisen constant. The bcc W phase has no pronounced phonon anomalies at normal pressure, but at high pressures (when it becomes thermodynamically unstable) several phonon modes soften, in particular the $L[\frac{2}{3}\frac{2}{3}\frac{2}{3}]$ and $T_{[1\bar{1}0]}[\frac{1}{2}\frac{1}{2}0]$ modes that are known to be soft in several other bcc transition metals. A related but less expected and more pronounced softening is noted in the $T_{[1\bar{1}0]}[\frac{1}{4}\frac{1}{4}0]$ mode, which also provides a path for bcc \rightarrow hcp transformation. This feature should be important for future studies of martensitic bcc-hcp transitions. The fcc W

phase is dynamically unstable under all shear at normal pressure. The unstable transverse phonon modes extend over such a large part of the BZ at $T = 0$ K and zero pressure that we do not expect fcc W to be stabilized at high T . However, with increasing pressure the phonons in fcc W tend to stabilize, and no instabilities remain when the volume has been reduced to about half of the volume at zero pressure.

This work was supported by the Swedish research councils NUTEK and NFR.

*Present address: National Renewable Energy Laboratory, Golden, Colorado 80401.

- [1] K.-M. Ho, C.-L. Fu, and B.N. Harmon, Phys. Rev. B **28**, 6687 (1983).
- [2] J. Trampenau, W. Petry, and C. Herzig, Phys. Rev. B **47**, 3132 (1993); W. Petry, thesis Dr. habil., Institut Laue-Langevin, France (1991).
- [3] P.J. Craievich, M. Weinert, J.M. Sanchez, and R.E. Watson, Phys. Rev. Lett. **72**, 3076 (1994).
- [4] P.J. Craievich, J.M. Sanchez, R.E. Watson, and M. Weinert, Phys. Rev. B **55**, 787 (1997).
- [5] V.L. Sliwko, P. Mohn, K. Schwarz, and P. Blaha, J. Phys.: Condens. Matter **8**, 799 (1996).
- [6] J.M. Wills, O. Eriksson, P. Söderlind, and A.M. Boring, Phys. Rev. Lett. **68**, 2802 (1992).
- [7] A. Fernández Guillermet, V. Ozoliņš, G. Grimvall, and M. Körling, Phys. Rev. B **51**, 10364 (1995).
- [8] F. Mauri, O. Zakharov, S. de Gironcoli, S.G. Louie, and M.L. Cohen, Phys. Rev. Lett. **77**, 1151 (1996).
- [9] *Landolt-Börnstein New Series*, edited by K.-H. Hellwege and J.L. Olsen (Springer-Verlag, Berlin, 1981), Vol. 13.
- [10] P. Hohenberg and W. Kohn, Phys. Rev. **136**, 864 (1964); W. Kohn and L.J. Sham, Phys. Rev. A **136**, 1133 (1965).
- [11] D.M. Ceperley and B.J. Alder, Phys. Rev. Lett. **45**, 566 (1980); J.P. Perdew and A. Zunger, Phys. Rev. B **23**, 5048 (1981).
- [12] A.M. Rappe, K.M. Rabe, E. Kaxiras, and J.D. Joannopoulos, Phys. Rev. B **41**, 1227 (1990).
- [13] H.J. Monkhorst and J.D. Pack, Phys. Rev. B **13**, 5188 (1976).
- [14] M. Methfessel and A.T. Paxton, Phys. Rev. B **40**, 3616 (1989).
- [15] S. Baroni, P. Giannozzi, and A. Testa, Phys. Rev. Lett. **58**, 1861 (1987); P. Giannozzi, S. de Gironcoli, P. Pavone, and S. Baroni, Phys. Rev. B **43**, 7231 (1991).
- [16] V. Ozoliņš, Ph.D. thesis, Royal Institute of Technology, Sweden (1996).
- [17] S. de Gironcoli, Phys. Rev. B **51**, 6773 (1995).
- [18] A. Larose and B.N. Brockhouse, Can. J. Phys. **54**, 1819 (1976).
- [19] A. Fernández Guillermet and G. Grimvall, Phys. Rev. B **44**, 4332 (1991).
- [20] C. Falter, W. Ludwig, W. Zierau, and M. Selmke, Phys. Lett. **93A**, 298 (1983).
- [21] W.A. Bassett and E. Huang, Science **238**, 780 (1987).
- [22] Y. Chen, K.M. Ho, and B.N. Harmon, Phys. Rev. B **37**, 283 (1988).